Supplementary Data for:

Bioactive Paper Dipstick Sensors for Acetylcholinesterase Inhibitors Based on Sol-Gel/Enzyme/Gold Nanoparticle Composites

Roger E. Luckham and John D. Brennan,*[a]

Received (in XXX, XXX) Xth XXXXXXXXX 200X, Accepted Xth XXXXXXXXX 200X
First published on the web Xth XXXXXXXXX 200X
DOI: 10.1039/b000000x

Presented below are background data on a new solid-phase colorimetric bioassay format based on enzyme catalyzed enlargement of gold nanoparticles (AuNP) that are co-entrapped with the enzyme in a sol-gel based silica material. Data are presented using acetylcholinesterase (AChE) as a model system. Test solutions containing acetylthiocholine (ATCh) and a Au(III) salt are added externally to silica materials containing AChE and small (3 nm diameter) AuNP, which are present within the wells of 96 well plates. Biocatalysed hydrolysis of ATCh *via* AChE leads to formation of thiocholine, which in turn reduces the Au(III) onto the entrapped nanoparticles, producing particle growth and a concomitant increase in color intensity that can be correlated to the amount of substrate or inhibitor present in test solutions. The data show that the entapped AuNP cannot leach from the silica material, leading to a solid-phase assay that has the potential to be integrated into a portable biosensing platform that can utilize visual detection of a color change as a simple readout. Our results show that the assay is sufficiently sensitive to allow for detection of Paroxon and aflatoxon B_1 with detection ranges of 3-10 μM and 15-1000 nM, respectively, when using a platereader for detection of color changes.

Introduction

In recent years a series of novel optical and electrochemical assays have been described based on the aggregation/deaggregation[1] or catalytic enlargement[2,3,4] of gold or other metal nanoparticles (NPs). In the first case, the biomolecule (usually DNA) is tagged with gold nanoparticles (AuNP), and addition of analyte leads to assembly or disassembly of NP labelled DNA, leading to a change in the distance of NPs and a color change. Nucleic acid functionalized semiconductor NPs have also been used as labels for the electrochemical,[5] optical,[6] or photoelectrochemical[7] detection of DNA and as a sensing platform for aptamer and DNAzyme based sensors.[8] It is also possible to integrate this assay into a lateral flow device to perform solid-phase aptamer or antibody based assays.[9]

More recently, the biocatalytic growth of AuNPs has been employed as a sensing mechanism. The catalytic reduction of metal ions onto NPs has been utilized extensively for "amplified" biosensing of antigen–antibody complexes,[10] DNA hybridization processes[11] and aptamer–protein binding.[8] The catalytic enlargement of AuNP-labeled DNA complexes between electrodes has also been used for conductivity-based biosensing of DNA.[12] An alternative sensing mechanism involves the enzyme-mediated reduction of metal ions onto NPs to cause particle growth to occur, which can be used for detection of enzymes, substrates or enzyme inhibitors.[2] There have been several reports of enzyme-mediated AuNP assays, including: the optical detection of NAD^+-dependent biocatalytic transformations based on the catalytic enlargement of AuNPs[2] by the reduction of Au(III)[13] or Cu(II)[14] with NAD(P)H cofactors; analysis of tyrosinase-generated neurotransmitters,[15] the detection of glucose either directly[16] or using an Os(III) mediator;[17] and the detection of AChE inhibitors using the thiocholine product to reduce Au(III) onto AuNPs that were immobilized onto glass slides.[18] Other metal salts, such as Ag(I), have also been utilized to allow detection of enzymatic reactions such as the hydrolysis of *p*-aminophenol phosphate by alkaline phosphatase to yield *p*-aminophenol, which catalyzes the reduction of Ag^+ onto Au NPs.[19]

While this method has been demonstrated for a variety of enzymes;[2] to date the assay has only been applied to enzymes in solution, and has not been demonstrated in a solid-phase assay format. The extension of this technology to solid-phase assays has significant potential for the development of a new class of colorimetric biosensors. The development of low-cost, portable and technically straightforward assay technologies is of critical importance in a number of areas, including rapid testing of food or water quality, point-of-care diagnostics (i.e. field or home setting), or the rapid detection of bioterror agents. Development of such bioassays could also be useful for performing routine analysis in underdeveloped countries, or as an alternative to more expensive technologies for rapid testing in emergency situations, since it is possible to detect a signal visually without the need for complex instrumentation.[20]

The development of portable, solid-phase colorimetric assays requires a method for immobilization of the biorecognition element (protein, DNA, etc) onto a suitable

substrate[21,22] as well as an appropriate method to generate a detectable color change. Toward this end, we have investigated the use of biocompatible sol-gel derived materials as a medium to co-entrap both an enzyme[23-28] and a small gold nanoparticle (colorimetric reagent) to allow for solid-phase assaying of enzyme substrates and inhibitors. Key issues in the assay development centered on finding conditions that would allow enzyme stimulated enlargement of gold nanoparticles within the pores of sol-gel materials, finding suitable conditions that would prevent the reduction of Au(III) by other assay components, and on optimizing this platform for solid-phase colorimetric assays.

As a starting point, we have utilized acetylcholinesterase (AChE) as the model enzyme. The enzyme has previously been shown to remain functional in sol-gel derived materials,[29] and can be used to catalyze the hydrolysis of acetylthiocholine to thiocholine, which has previously been shown to reduce Au(III) onto AuNPs.[18] This enzyme is also important as a biorecognition element for detection of organophosphates, which can be used as pesticides or biowarfare agents,[30] and for detection of aflatoxins,[31] which is a biomarker of food spoilage.[32] Herein we describe the optimization of assay conditions to achieve the best assay performance, and show the quantitative detection of both substrates and inhibitors of AChE using the colorimetric sol-gel derived solid-phase assay platform.

Experimental

Materials

Sodium silicate solution (SS, ~14% NaOH, ~27% SiO_2), Dowex 50WX8-100 ion-exchange resin, acetylcholinesterase (AChE, from *Electrophorus electricus*, EC 3.1.1.7), acetylthiocholine iodide (ATCh), gold(III)chloride trihydrate, adenosine 5′-triphosphate disodium salt (ATP), diethyl 4-nitrophenyl phosphate (Paraoxon) and Aflatoxin B_1 (AFB_1) were obtained from Sigma-Aldrich. Costar® 96-well half-area plates were obtained from Fisher Scientific. Distilled deionized water was obtained from a Milli-Q Synthesis A10 water purification system. All reagents were used as received.

Safety Precautions

NOTE: Paraoxon and aflatoxin B_1 are extremely toxic compounds. Stock solutions of these compounds were handled in a designated fume-hood with appropriate personal safety equipment, including gloves, masks and safety glasses. These were employed at all times when handling these substances.

Procedures

Preparation of ATP-Capped Gold Nanoparticles

ATP-AuNPs were prepared as described by Zhao *et al.*[33] Briefly, 60 µL of 10 mM gold chloride solution was added to 60 µL of a 10 mM ATP solution. To this, 2.75 mL of deionized water was added followed by shaking and incubation for 30 minutes at room temperature. 100 µL of freshly prepared 0.01 M $NaBH_4$ solution was then added and the resulting solution was shaken for 10 seconds followed by incubation at room temperature for 3 hrs. The resulting solution of nanoparticles had a mean diameter of 2-3 nm, and could withstand up to 1 M NaCl without aggregation.

Preparation of Sol-Gel Materials

Sodium silicate sols were prepared by mixing 10 mL of ddH_2O with 2.9 g of sodium silicate solution (pH ~13) followed by addition of 5 g of Dowex cation exchange resin to replace Na^+ with H^+. The mixture was stirred for 30 seconds to reach a final pH of ~4, and then vacuum filtered through a Büchner funnel. The filtrate was then further filtered through a 0.45 µM membrane syringe filter to remove any particulates in the solution.

ATP-AuNPs (volume of 0 – 4 µL) were added to the sodium silicate (SS) precursor sol to acheive a final volume of 50 µL, which was then mixed in a 1:1 volume ratio with a buffered solution (100 mM Tris-HCl, pH 8.0) containing AChE at room temperature (20 ± 1 °C) to provide a final volume of 100 µL of material in the well of 96-well plate, with a final enzyme concentration of 0 – 50 $Units.mL^{-1}$ (1 Unit = 1 µmole of acetylcholine hydrolyzed per min at 37 °C). In all assays, 30 µL of the AChE/ATP-AuNP doped silica sol was allowed to gel and cure for 72 hrs at 4 °C prior to performing assays. Note: The concentrations of ATP-AuNP were calculated based on a molar extinction coefficient (ε_{550}) of 6.5 x 10^5 $M^{-1}cm^{-1}$ for particles on the order of 2-3 nm, as reported by Pavlov *et al.*[8]

Optimization Studies

A series of different sol-gel derived silica materials containing varying levels of AChE and ATP-AuNPs were prepared as described above. The 30 µL gels were then allowed to cure for 72 hours at 4 °C. In all cases, 30 µL of a solution containing varying levels of ATCh and gold chloride was added to the wells and left for 1 h at room temperature while shaking. Controls included materials with no AChE or no AuNPs and the use of solutions with no ATCh or no gold chloride to ensure that any color changes were due to enzyme catalyzed enlargement of AuNPs within the silica. After 1 h the absorbance spectra of the materials were measured from 400 nm to 900 nm using a TECAN Safire microwell plate reader. The absorbance at 550 nm was plotted against the concentration of the various reagents (AChE, ATCh, Au(III) or AuNP) to determine the effect of reagent concentration on signal and background levels.

Inhibition Assays

To the 30 µL AChE/ATP-AuNP doped silica monoliths, 10 µL of inhibitor solution was over spotted and incubated at room temperature while shaking for 1 h. 20 µL of a solution containing appropriate concentrations of Au(III) and ATCh along with an identical concentration of inhibitor (to avoid dilution of inhibitor) was then added and shaken for 1 h. Absorbance was then measured using a TECAN Safire microwell plate reader. The absorbance at 550 nm was plotted against inhibitor concentration to derive IC_{50} plots.

Long Term Stability Studies

Microwell plates containing the AChE and AuNP doped silica materials were sealed with Parafilm® and stored at 4 °C for up to 90 days. 30 µL of a test solution containing the optimized amounts of ATCh and Au(III) were then added at various time points, the plate was shaken for 1 h and absorbance measurements were obtained using a TECAN Safire microwell plate reader. Activity was referenced to that obtained from a sample that had been aged for 3 days.

Transmission Electron Microscopy

ATP-AuNP doped silica materials were imaged by TEM before and after enzyme assays to determine the extent of particle growth during assays. Samples of approximately 0.5 g were immersed in 500 µL methanol and sonicated for 30 min at room temperature. Samples were then dried and immediately placed on a TEM grid for imaging. Images were acquired using a JEOL Ltd. (Tokyo, Japan) JEM-1200EX instrument operating at 80 kV.

Results and discussion

Proof of Concept

The choice of gold nanoparticles is of particular importance in this work for two reasons: the primary nanoparticles must (1) be able to withstand relatively high buffer salt concentrations (~50 mM) as is commonly used when entrapping proteins within sol-gel derived silica materials and (2) be biocompatible in the sense that these will not degrade the biological component(s) in any way. A solution-based AuNP assay for the detection of AChE inhibitors was previously described by Pavlov and coworkers[8] where citrate capped AuNPs were employed as the platform for particle growth. As a starting point, a similar protocol[33] was used in this work, however it was discovered that the citrate capped AuNPs were very sensitive to increasing salt concentration, with significant aggregation occurring above 5 mM (data not shown), which made it difficult to develop reproducible assays. The primary AuNPs provide the physical platform upon which elemental gold is deposited – resulting in particle growth. Hence, it is important that the primary particles remain in a non-aggregated form within the matrix. As a result of the relative instability of the citrate capped AuNPs to salt, a more stable primary AuNP was required. To achieve this goal, we utilized highly stable, biocompatible AuNPs in which ATP was used as the capping agent.[33] These nanoparticles showed good stability, with no aggregation occurring even at buffer salt concentrations of approaching 1.0 M, and were therefore used for all solution and solid-phase assays.

The general reaction scheme for the AChE catalyzed growth of ATP-capped AuNPs in the solid-phase assay is shown in Figure S1. In this assay, 2-3 nm primary AuNPs and AChE are co-entrapped in a silica matrix which is present in a microwell of a 96-well plate. Solutions containing inhibitor

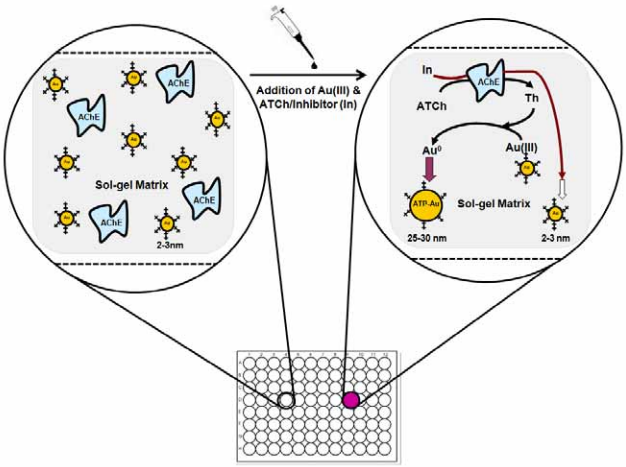

Fig. S1 Schematic of the solid-phase assay involving enzymatically catalyzed enlargement of entrapped gold nanoparticles.

and ATCh/Au(III) are introduced and these reagents are able to diffuse into the silica matrix. AChE catalyzed hydrolysis of the ATCh substrate results in the production of thiocholine, which is able to reduce Au(III) onto the entrapped AuNPs. This causes enlargement of the AuNPs to a diameter of 25-30 nm or greater and a concomitant increase in absorbance and color intensity. It is important to note that materials that do not contain primary AuNPs do not produce a color change; the co-entrapped AuNPs are necessary in order to produce nucleation sites for rapid particle growth (see below).

As a starting point for assay development, we set out to demonstrate that it was possible to perform enzymatically catalyzed enlargement of primary AuNPs within the pores of a sol-gel derived silica matrix. For this purpose, AChE and ATP-AuNPs were entrapped in a biocompatible silica matrix derived from sodium silicate and the Au(III) and ATCh solutions were added externally. Sodium silicate was chosen as it is an easily prepared, optically transparent, biocompatible silica precursor that is known to maintain the activity of enzymes,[34] and does not produce byproducts (i.e. alcohols, glycerol, etc) that might interfere with the growth of AuNPs.

Figure S2 shows an image of a microwell plate in which a series of solid-phase assays and control experiments were performed. The original image was processed using ImageJ to enhance the contrast and brightness and increase the color saturation. No other processing was performed. The top row (A1-A7) shows the ATP-AuNP and AChE doped silica before addition of substrate and gold chloride. In this case, the samples are completely colorless and transparent, showing that the low concentration of small ATP-AuNPs does not produce a significant background absorbance. Absorbance measurements of the wells performed using a TECAN Safire platereader confirmed this as the characteristic plasmon absorbance band for AuNP, between 510 and 550 nm, was not detectable (data not shown). Wells B1-E1 show control experiments in which silica materials were formed or assays were run with one of the assay components missing; AChE (B1), ATCh (C1), Au(III) (D1) or entrapped primary AuNPs (E1). All other reagents were present at the highest concentrations used in the assay, which are present in the last

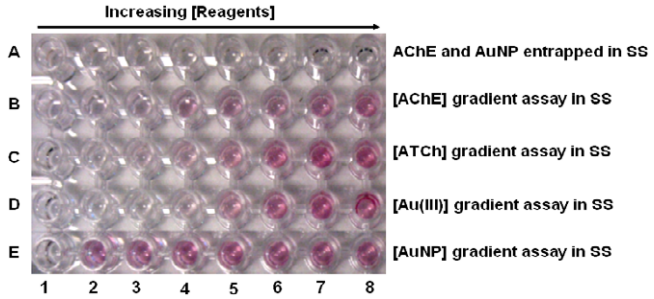

Fig. S2 Proof of concept and control experiments for the solid-phase bioassay (showing that all reagents are necessary for nanoparticle growth). Wells were filled with sol-gel derived materials containing the reagents indicated. A: Appearance of well before over spotting of ATCh and Au(III); B: Assay of varying [AChE] (0 to 40 unit/mL) at constant [ATCh], [Au(III)] and [ATP-AuNP]. C: Assay of varying [ATCh] (0 to 0.45 mM) at constant [AChE], [Au(III)] and [ATP-AuNP]. D: Assay of varying [Au(III)] (0 to 0.83 mM) at constant [AChE], [ATCh] and [ATP-AuNP]. E: Assay of varying [ATP-AuNP] (0 to 1x 4 conc. units) at constant [AChE], [ATCh] and [Au(III)].

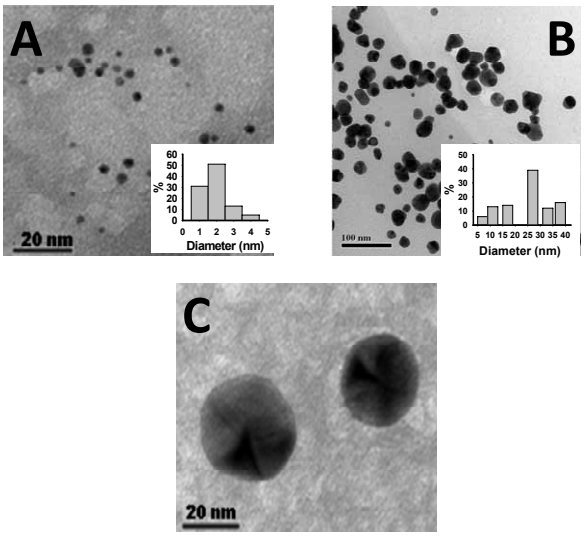

Fig. S3 TEM Images of ATP-AuNPs within sol-gel derived silica before (Panel A) and after (Panel B) performing the solid-phase enzyme assay. Inset: ATP-AuNP size distribution charts. Panel C shows ATP-AuNPs after assay at a lower magnification (5 X), relative to Panel B.

column (B7-E7). In all cases, there was no change in the color of the material, indicating that the silica material and assay reagents (i.e., buffer salts, substrates, etc) did not cause significant reduction of Au(III) or conversion of ATCh to a product that could promote reduction of Au(III) and subsequent enlargement of primary AuNPs.

Row B shows the effect of increasing AChE concentration on the reaction. Here it is seen that as the concentration of AChE is increased from 0 to 40 unit/mL (B1-B7), a color gradient is formed as the concentration of AChE is increased. For this assay the concentration of ATP-AuNP, Au(III) and ATCh were kept constant. This assay establishes that the presence of the highest level of AChE produced the largest change in color, indicative of the greatest extent of enlargement of the entrapped AuNPs. These experiments also conclusively demonstrate that ATP-capped AuNPs can be bio-catalytically grown within the confines of a sol-gel matrix and also show that the growth of AuNPs is due to the activity of the entrapped enzyme and not due to background interferences related to the sol-gel material or other components of the reaction mixture.

Row C of Figure S2 shows assays involving increasing amounts of ATCh incubated over the silica material; as in the case with the AChE gradient assay, there was also a progression of colour that was formed, from low to high, as the concentration of ATCh was increased. A similar trend was observed for rows D and E, where the concentration of Au(III) and ATP-AuNP was varied. This demonstrates that the presence of all reagents is necessary for signal generation, and that color intensity increases with the concentration of each assay reagent, as expected.[18] Hence, this system provides a suitable platform for a colorimetric solid-phase assay.

TEM Imaging

To confirm that the color changes were the result of entrapped nanoparticle growth, AChE/AuNP doped silica monoliths were imaged by TEM before and after performing a solid-phase AChE assay. Microtoming is a common sample preparation technique used when taking TEM images of materials such as these. However, microtoming requires that the sample be completely devoid of moisture, meaning that the sol-gel material would have to be desiccated. Dehydration of bulk gels resulted in significant shrinkage, which lead to aggregation of entrapped AuNPs, producing images that were not representative of the particle size within hydrated silica materials. To make samples amenable to TEM, they were first immersed in methanol with sonication to remove water and soluble organic components, and then placed on TEM grids and dried. Figure 3 shows the TEM images obtained before (Fig S3A) and after (Fig. S3B) performing the enzymatic assay. As shown in the inset distribution plot Figure S3A, the average particle size for AuNPs was 2 nm with few particles above 4 nm in diameter prior to performing the assay. After performing the assay there are large numbers of metal nanoparticles that have sizes ranging from 5 – 40 nm, (Fig S3B) clearly indicating growth of the nanoparticles within the silica matrix As shown in the inset distribution plot, the average particle size was ~25 nm, with 65% of particles in the size range from 25 – 40 nm in diameter (Fig. 3B). As shown in Fig. S3C, the entrapped particles show relatively regular spherical shapes after enlargement, indicating that the matrix does not preclude formation of large particles that can produce significant color changes. Thus, the enlarged particles can be used for visual detection of the enzymatic reaction using this solid-phase assay platform.

Optimization of Solid-Phase Assay

To optimize the reagents for the assay, AChE/ATP-AuNP doped silica materials were prepared with varying concentrations of AChE and ATP-AuNPs, and were assayed using varying concentrations of ATCh and Au(III). Figure 4A-D shows the results obtained when each of the four components was varied systematically with the other three reagent concentrations was

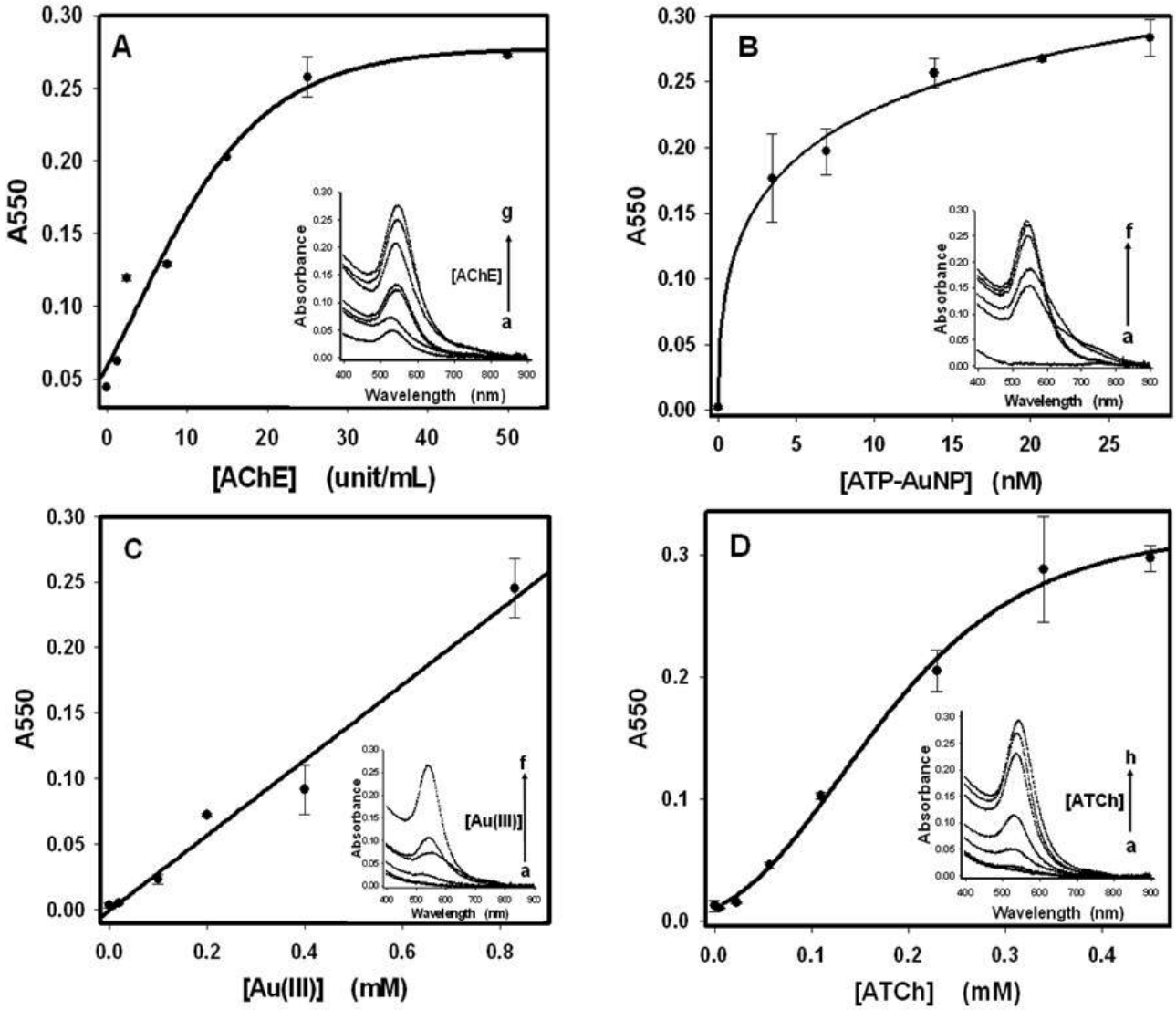

Fig. S4 (A) Inset: Normalized absorption spectra showing the effect of [AChE] on the growth of ATP-AuNPs in a SS derived sol-gel (SG) matrix. [AChE]: (a) 0 unit/mL; (b) 1.25 unit/mL; (c) 2.50 unit/mL; (d) 7.5 unit/mL; (e) 15.0 unit/mL; (f) 25.0 unit/mL; (g) 50.0 unit/mL. In all assays the system includes: [ATCh] = 0.45 mM; [Au(III)] = 0.83 mM; [ATP-AuNP] = 28 nM. (B) Inset: Normalized absorbance spectra showing the effect of [ATP-AuNP] on the signal achieved at constant [AChE], [Au(III)] and [ATCh]: 50.0 unit/mL, 0.83 mM and 0.45 mM respectively. [ATP-AuNP]: (a) 0 nM; (b) 3.5 nM (c) 6.9 nM (d) 14 nM; (e) 21 nM (f) 28 nM. (C) Inset: Normalized absorption spectra showing the effect of [Au(III)] on the growth of ATP-AuNPs in a SS derived SG matrix. [Au(III)]: (a) 0 mM; (b) 0.02 mM; (c) 0.10 mM; (d) 0.20 mM; (e) 0.40 mM; (f) 0.83 mM. In all assays the system includes: [ATCh] = 0.45 mM; [AChE] = 50.0 unit/mL; [ATP-AuNP] = 28 nM (D) Inset: Normalized absorbance spectra showing the effect of [ATCh] on the growth of ATP-AuNPs at constant [AChE], [Au(III)] and [ATP-AuNP]: 50.0 unit/mL, 0.83 mM and 28 nM respectively. [ATCh]: (a) 0 mM; (b) 0.0056 mM; (c) 0.023 M; (d) 0.057mM; (e) 0.11 mM; (f) 0.23 mM; (g) 0.34 mM; (h) 0.45 mM .

held constant. All assays were run for a period of 1 h, after which an absorbance spectrum was obtained. Figure S4A shows the effect of varying the concentration of entrapped AChE from 0 – 50 Unit/mL when using constant concentrations of AuNP (28 nM), ATCh (0.45 mM) and Au(III) (0.83 mM). The data show that the absorbance increases linearly as the concentration of AChE is increased up to 25 Unit/mL, and then levels off, suggesting that higher levels of AChE may lead to aggregation of the enzyme and loss of activity. The inset of Figure S4A shows the absorbance spectra obtained for the reaction run at different AChE concentrations. This plot clearly shows an increase in the characteristic plasmon absorbance band, which provides strong evidence for growth of the entrapped AuNPs. An important point is that the signal level is not zero when AChE is absent; this likely reflects slow autohydrolysis of the ATCh with a concomitant reduction of Au(III) to produce an increase in absorbance.

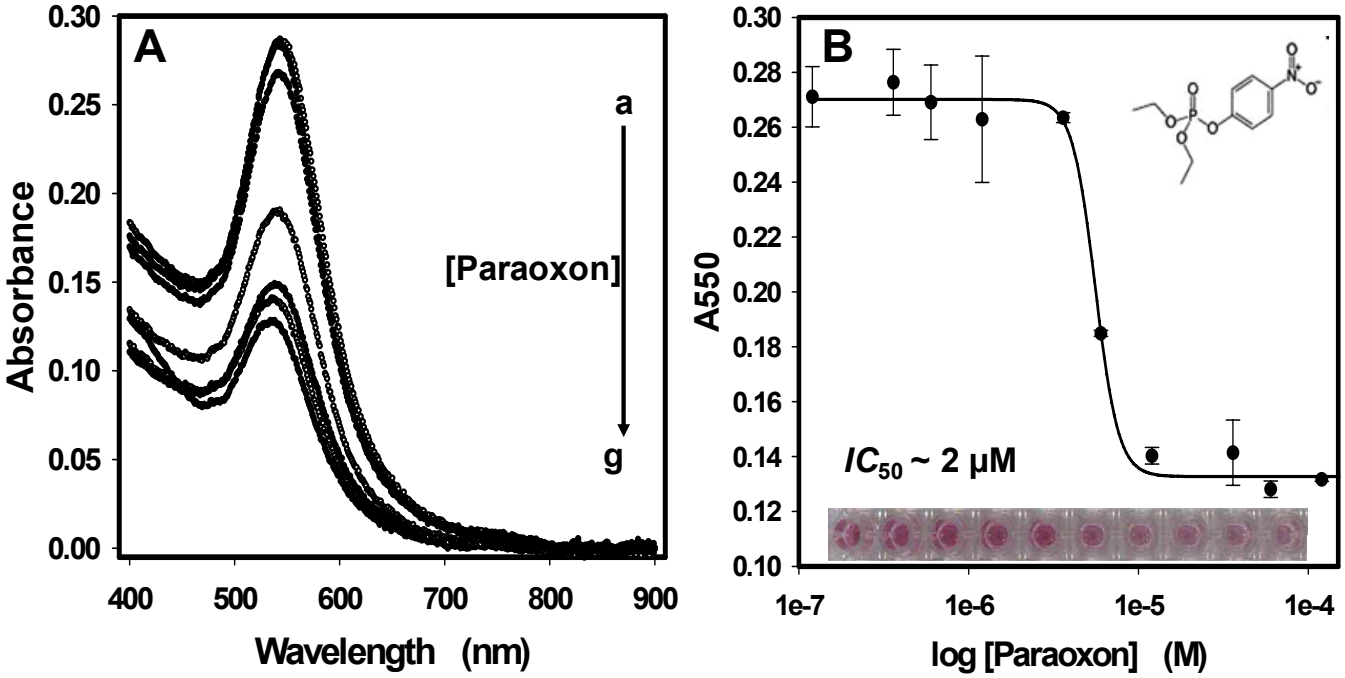

Fig. S5 (A) Absorbance spectra showing the effect of Paraoxon on the growth of ATP-AuNPs. [Paraoxon]: (a) 0 M; (b) 4.0 x 10^{-8} M; (c) 4.0 x 10^{-7} M; (d) 1.0 x 10^{-6} M; (e) 2.0 x 10^{-6} M; (f) 4.0 x 10^{-6} M; (g) 4.0 x 10^{-5} M. Note: Overlapping spectrum were not included for sake of clarity. (B) Corresponding IC_{50} plot for Paraoxon as determined *via* solid phase enzyme assay. All assays include: AChE, 50.0 unit/mL; ATCh, 0.45 mM; Au(III), 0.83 mM; and ATP-AuNP; 28 nM.

Figure S4B shows the effect of the concentration of entrapped AuNPs at a constant concentration of AChE (50 Units/mL), ATCh (0.45 mM) and Au(III) (0.83 mM). Once again, the signal increases asymptotically with the concentration of added reagent, and in this case clearly shows that systems that do not contain entrapped AuNPs do not produce any discernable signal while systems with high levels of AuNPs (on the order of 28 nM) provide large color changes. The data demonstrate that primary AuNP particles are necessary to support growth of larger particles; systems that do not contain primary particles cannot support particle growth upon reduction of Au(III) and hence provide no color change. Interestingly, the shape of the absorbance spectra change with the concentration of entrapped AuNPs. Assays in which higher concentrations of primary AuNPs are present show sharper plasmon absorbance bands, likely reflecting more homogenous particle growth. Figure 4C shows the effect of Au(III) concentration on signal levels, with constant levels of AChE (50 unit/mL), ATCh (0.45 mM) and AuNP (28 nM). In this case the signal changes linearly with the concentration of Au(III), and does not approach a saturation level. The experiment was terminated at 0.83 mM as there was a significant background gold color present above this level which made it difficult to detect the color change by eye. Once the other reagents were optimized, the effect of substrate concentration on absorbance was evaluated by varying the concentration of ATCh at constant levels of AChE (50 unit/mL), AuNP (28 nM) and Au(III) (0.83 mM). The response was in general agreement with the expected Michaelis-Menten response (though it must be noted that we plot an endpoint value after 1 h rather than a rate), with the signal showing saturation at 0.45 mM. The experimental apparent K_M value for ATCh is ~150 µM, which is in good agreement with the literature value of 140 µM obtained from AuNP based solution assays.[18] The lag in response at very low ATCh concentrations may reflect mass transfer limitations and/or issues with partitioning of the cationic substrate into the sol-gel material, which have been previously observed for enzymes entrapped in sol-gel materials.[35]

Inhibition Assays

It is well known that AChE can be inhibited by a range of compounds, including organophosphates, aflatoxins, carbamates and compounds such as galanthamine and sanguinine, which are often used as therapeutics for treatment of Alzheimer's disease.[36] For the purposes of this work however, the organophosphate Paraoxon and the mycotoxin Aflatoxin B_1 (AFB_1) were investigated. The choice of target analytes allows us to assess the potential of the solid-phase assay as a tool to detect species that are potential bioterror agents (organophosphates)[37] and biomarkers for food spoilage.[31,38,39]

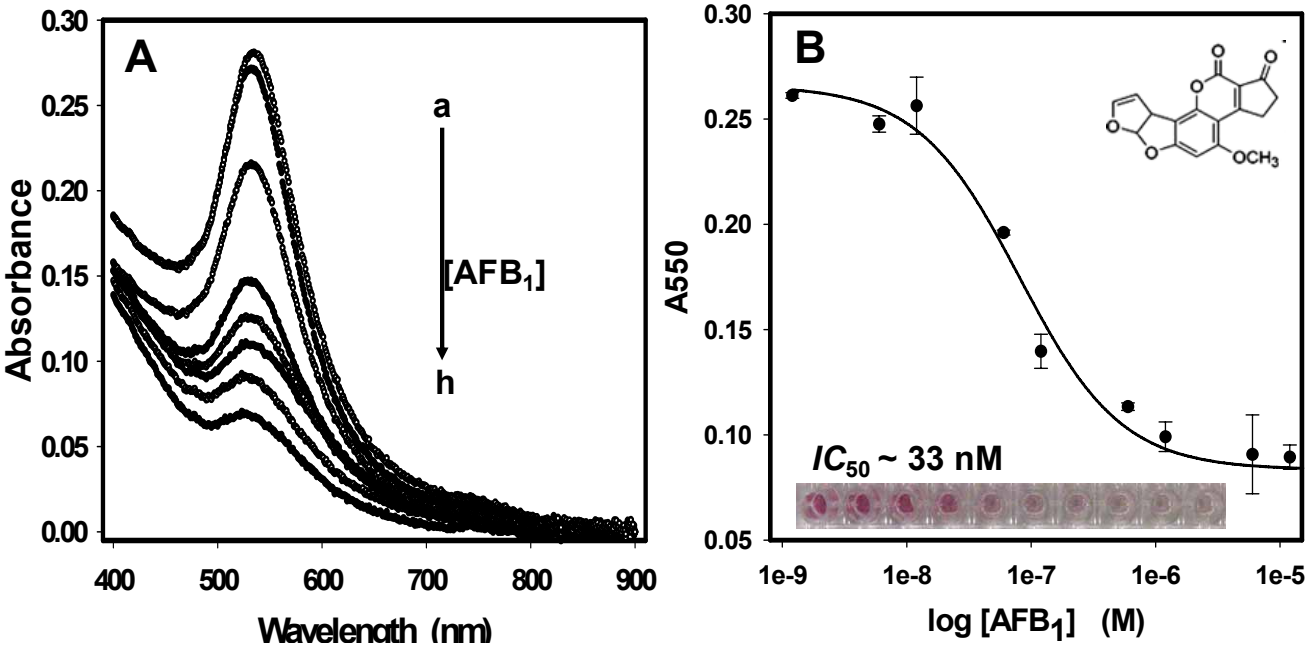

Fig. S6 (A) Absorbance spectra showing the effect of AFB_1 on the growth of ATP-AuNPs. [AFB_1]: (a) 0 M; (b) 4.0 x 10^{-10} M ; (c) 4.0 x 10^{-9} M; (d) 2.0 x 10^{-8} M ; (e) 4.0 x 10^{-8} M; (f) 2.0 x 10^{-7}M; (g) 4.0 x 10^{-7} M; (h) 2.0 x 10^{-5} M. Note: Overlapping spectrum were not included for sake of clarity. (B) Corresponding IC_{50} plot for Aflatoxin B_1 as determined *via* the solid phase enzyme assay. All assays include: AChE, 50.0 unit/mL; ATCh, 0.45 mM; Au(III), 0.83 mM; and ATP-AuNP, 28 nM.

Inhibition assays for each of the target molecules were performed by adding 10 µL of a solution containing the appropriate concentration of analyte to the AChE/AuNP doped silica materials followed by incubation for 1 h. 20 µL of a solution containing optimum concentrations of ATCh and Au(III) along with the inhibitor at its original concentration was then added and incubated for 1 h to allow for proper diffusion into the sensor and signal generation, after which absorbance was measured. The sensitivity of SS entrapped AChE to inhibition by Paraoxon and Aflatoxin B_1 was assessed by determination of 50% inhibitory concentrations (IC_{50}). Figure 5A shows the absorbance spectra for inhibition assays in which the concentration of Paraoxon was varied from 0 to 4.0 x 10^{-5} M (spectrum a to g). Here it is seen that as the concentration of inhibitor is increased, the plasmon absorbance band decreases in amplitude. This clearly demonstrates that AChE is being inhibited, causing a reduction in the growth of AuNP. The IC_{50} for Paraoxon was calculated to be 1.9 ± 0.1 µM (Figure5B), which is in agreement with the literature value of 0.7 - 3.1 µM.[37] Figure S6A shows the absorbance spectra for assays in which the concentration of AFB_1 was varied from 0 to 2.0 x 10^{-5} M (spectrum a to h). Similar to the Paraoxon assay, as the concentration of the mycotoxin increased the corresponding plasmon absorbance band decreased. The IC_{50} for AFB_1 was calculated to be 33.1 ± 4.7 nM (Figure S6B), which was somewhat lower than the literature value of 192 nM.[31] As demonstrated by Besanger *et al.*[35] sol-gel entrapment can alter the IC_{50} values for enzyme inhibitors owing to mass transfer and/or partitioning effects. The data suggest that the AFB_1 compound preferentially partitions into the sol-gel film.

While IC_{50} values are useful for determining the potency of the inhibitor, in the case of pesticide and mycotoxin detection, the comparison of limit of detection (LOD) to toxicity (LD_{50}) of specific inhibitors is more applicable. The LD_{50} for Paraoxon in relation to rats, as reported by manufacturer's MSDS is 6.5 µM (1.8mg/kg), while the LOD for Paraoxon (S/N = 3) as determined by our solid phase assay platform was calculated to be 3 µM. The LD_{50} for AFB_1 has been reported to be 1.5 µM, although the legal limits for AFB_1 are normally in the range of 10 – 700 nM;[40] the LOD for this compound using the solid phase assay was 15 nM. Thus, the detection limits of the inhibitors were found to be less than the reported LD_{50} towards rats (orally administered) and in line with the lowest legislated limits. Hence, it is clear that the sol-gel based, solid phase bioassay platform is sufficiently sensitive, as it can detect sub-lethal concentrations of these compounds.

Long Term Stability

A potential benefit of immobilized enzymes is their resistance to denaturation.[23] A number of enzymes, including AChE,[41] have been shown to possess excellent long term stability when entrapped within sol-gel derived silica materials. However, no studies exist relating to the stability of the primary AuNPs within the silica matrix, and thus was important to assess the stability of this sensing platform. For this purpose, the AChE/AuNP-doped silica materials were stored at 4 °C for 90 days, with assays performed on a weekly basis. These experiments indicated that AChE retained full activity and the AuNPs retained their ability to grow and produce color changes over 90 days (see Fig 5). Previous studies of

entrapped enzymes have shown that some enzymes, such as Factor Xa, can remain active in sol-gel derived materials for several months.[35] Hence, it is likely that the AChE/AuNP solid-phase assay platform should have a useful shelf life.

Conclusions

The data show that it is possible to enzymatically catalyze the growth of primary AuNPs from 3 nm to > 30 nm in diameter when a suitable enzyme is co-entrapped with the AuNPs within the pores of sol-gel derived silica materials, and that this process can be coupled to a large change in absorbance, which can be used to detect enzyme substrates or inhibitors. The bioassay demonstrated herein was based on acetylcholinesterase (AChE) catalyzed enlargement of gold nanoparticles, which resulted from reduction of Au(III) by the product thiocholine. However, a wide range of different enzyme catalyzed reactions are amenable to this general assay format, including several redox enzymes, NAD^+-dependent biocatalytic transformations, and alkaline phosphatase catalyzed reactions. Thus, the soild-phase colorimetric assay platform should have good versatility.

Our results show that the assay is sufficiently sensitive to allow for detection of pesticides (Paraoxon) and toxins (Aflatoxin B_1) with detection limits that are in good agreement with the expected IC_{50} values. Observed detection limits are below the LD_{50} threshold for both compounds, suggesting that the solid phase assay should easily detect sub-lethal levels of these compounds. The ability to visually detect the color change, and the inability of the AuNPs to leach from the solid matrix make this assay format amenable to remote testing without the need for complex instrumentation.

Acknowledgements

The authors thank the Natural Sciences and Engineering Research Council of Canada for funding this work through a network grant – *SENTINEL* Canadian Network for the Development and Use of Bioactive Paper. The authors also thank the Canada Foundation for Innovation and the Ontario Innovation Trust for support of this work. JDB holds the Canada Research Chair in Bioanalytical Chemistry.

Notes and references

[a] *Department of Chemistry, McMaster University, 1280 Main St. West, Hamilton, ON, L8S 4M1, Canada.. Fax:+1-905-527-9950; Tel:+1-905-525-9140 x. 27033; E-mail: brennanj@mcmaster.ca*

† Electronic Supplementary Information (ESI) available: [details of any supplementary information available should be included here]. See DOI: 10.1039/b000000x/

1 R. Elghanian, J.J. Storhoff, R.C. Mucic, R.L. Letsinger, C.A. Mirkin, *Science,* 1997, **277,** 1078-1080.
2 I. Willner, R. Baron, B. Willner, *Adv. Mater.,* 2006, **18,** 1109-1120.
3 S.K. Ghoah, T. Pal, *Chem. Rev.* 2007**, 107**, 4797-4862
4 M.-C. Daniel, D. Astruc, *Chem. Rev.* 2004, **104**, 293-346
5 J. Wang, G. Liu, R. Polsky, A. Merkoci, *Electrochem. Commun.,* 2002, **4,** 722-726; J. Wang, G. Liu, A. Merkoci, *J. Am. Chem. Soc.,* 2003, **125,** 3214-3215; J. Wang, D.K. Xu, A.N. Kawde, R. Polsky, *Anal. Chem.,* 2001, **73,** 5576-5581.
6 M. Bruchez, M. Moronne, P. Gin, S. Weiss, A.P. Alivisatos, *Science,* 1998, **281,** 2013-2016; W.C.W. Chan, S. Nie, *Science,* 1998, **281**, 2016-2018.
7 I. Willner, F. Patolsky, J. Wasserman, *Angew. Chem. Int. Ed.,* 2001, **40,** 1861-1864.
8 V. Pavlov, Y. Xiao, B. Shlyahovsky, I. Willner, *J. Am. Chem. Soc*., 2004, **126,** 11768 –11769.
7 J. Liu, D. Mazumdar, Y. Lu, *Angew. Chem. Int. Ed.,* 2006, **45,** 7955-7959.
10 O.O. Velev, E.W. Kaler, *Langmuir,* 1999, **15,** 3693 –3698; Y.C. Cao, R. Jin, J.-M. Nam, C.S. Thaxton, C.A. Mirkin, *J. Am. Chem*. Soc., 2003, **125,** 14676-14677; K. Faulds, W.E. Smith, D. Graham, *Anal. Chem*., 2004, **76,** 412 –417.
11 J. Wang, O. Rincon, R. Polsky, E. Dominguez, *Electrochem. Commun*., 2003, **5,** 83–86; J.M. Nam, C.S. Thaxton, C.A. Mirkin, *Science,* 2003, **301,** 1884–1886.
12 S.J. Park, T.A. Taton, C.A. Mirkin, *Science,* 2002, **295,** 1503–1506.
13 Y. Xiao, V. Pavlov, S. Levine, T. Niazov, G. Markovitch, I. Willner, *Angew. Chem*., 2004, **116,** 4619–4622; *Angew. Chem. Int. Ed*., 2004, **43,** 4519–4522.
14 B. Shlyahovsky, E. Katz, Y. Xiao, V. Pavlov, I. Willner, *Small,* 2005, **1,** 213-216.
15 R. Baron, M. Zayats, I. Willner, *Anal. Chem.,* 2005, **77,** 1566-1571.
16 M. Zayats, R. Baron, I. Popov, I. Willner, *Nano Lett.,* 2005, **5,** 21-25.
17 Y. Xiao, V. Pavlov, B. Shlyahovsky, I. Willner, *Chem. Eur. J.,* 2005, **11,** 2698-2704.
18 V. Pavlov, Y. Xiao, I. Willner, *Nano Lett.,* 2005, **5,** 649-653.
19 B. Basnar, Y. Weizmann, Z. Cheglakov, I. Willner, *Adv. Mater.,* 2006, **18**, 713-718.
20 A.W. Martinez, S.T. Phillips, M.J. Butte, G.M. Whitesides, *Agnew. Chem. Int. Ed.,* 2007, **46**, 1318-1320.
21 J.A. Camarero, *Biophys. Rev. Lett.,* 2006, **1,** 1-28.
22 D.A. Di Giusto, G.C. King, *Top. Curr. Chem.,* 2006, **261,** 131-168.
23 W. Jin, J.D. Brennan, *Anal. Chim. Acta*, 2002, **461,** 1-36.
24 I. Gill, *Chem. Mater.,* 2001, **13**, 3404-3421.
25 D. Avnir, T. Coradin, O. Lev. J. Livage, *J. Mater. Chem.,* 2006, **16,** 1013–1030.
26 A.C. Pierre, *Biocat. Biotrans.,* 2004, **22**, 145-170.
27 T. Coradin, M. Boissiere, J. Livage, *Curr. Med. Chem.,* 2006, **13**, 99-108.
28 T.R. Besanger, J.D. Brennan, *J. Sol-gel Sci. Technol.,* 2006, **40,** 209-225.
29 K. Anitha, S.V. Mohan, S.J. Reddy, *Biosens. Bioelectron*., 2004, **20,** 848-856; R.-A. Doong, H.-C. Tsai, *Anal. Chim. Acta,* 2001, **434,** 239-246; D. Du, S. Chen, J. Cai, A. Zhang, *Biosens. Bioelectron.,* 2007, 2007, **23**, 130-134.
30 T.C. Marrs, *Pharmacol. Ther.*, 1993, **58**, 51-66.
31 F. Arduini, I. Errico, A. Amine, L. Micheli, G. Palleschi, D. Moscone, *Anal. Chem.,* 2007, **79**, 3409-3415.
32 H.S. Hussein, J.M. Brasel, *Toxicology,* 2001, **167**, 101-134.
33 W. Zhao, F. Gonzaga, Y. Li, M.A. Brook, *Adv. Mater.,* 2007, **19**, 1766–1771.
34 R. B. Bhatia, C. J. Brinker, A. K. Gupta and A. K. Singh, *Chem. Mater.,* 2000, **12**, 2434-2441.
35 T.R. Besanger, Y. Chen, A.K. Deisingh, R. Hodgson, W. Jin, S. Mayer, M.A. Brook, J.D. Brennan, *Anal. Chem.,* 2003**, 75**, 2382-2391.
36 D. Wilkinson, J. Murray, *Int. J. Geriatric Psych.,* 2001, **16**, 852-857.
37 J.H. Skerritt, S.L. Guihot, M.B. Asha, B.E.A. Rani, N.G.K. Karanth, *Food Agric. Immun.,* 2003, **15,** 1-15.
38 H.S. Hussein, J.M. Brasel, *Toxicology,* 2001, **167**, 101-134.
39 S.M.Z Hossain, R.E. Luckham, A.M. Smith, J.M. Lebert, L.M. Davies, R.H. Pelton, C.D.M. Filipe, J.D. Brennan, *Anal. Chem.*, 2009, **81**, 5474–5483.
40 B.S. Delmulle, S.M.D.G. De Saeger, L. Siba, I. Barna-Vetro, C.H. Van Peteghem, *J. Agric. Food Chem.,* 2005, **53**, 3364-3368.
41 P.C. Pandey, S. Upadhyay, H.C. Pathak, C.M.D. Pandey, I. Tiwari, *Sens. Actuators B,* 2000**, 62**, 109–116.